

# **Influence of East Asia Pacific Teleconnection and Scandinavian Teleconnection on Summer Precipitation in Southwest China**

Yang Mingxin<sup>1,2</sup>, Xiao Tiangui<sup>1,2</sup>, Zhao Ping<sup>2</sup>, Li Yong<sup>3</sup>, Huang Wei<sup>4</sup>, Li Yueqing<sup>5</sup>,  
Tan Jie<sup>1</sup>

1 Chengdu University of Information Technology, Chengdu, 610225, China

2 Chinese Academy of Meteorological Sciences, Beijing, 100081, China

3 National Meteorological Centre, Beijing, 100081, China

4 Yunnan Climate Center, Kunming, 650034, China

5 Institute of Plateau Meteorology, CMA, Chengdu, 610072, China

**Abstract:** Based on the summer precipitation data of 328 stations in Southwest China in 50 years and the reanalysis data of NCEP / NCAR monthly geopotential height field, and wind field, the relationship between summer precipitation in Southwest China and East Asia Pacific teleconnection pattern (EAP) and Scandinavian teleconnection pattern (SCA) is explored by using EOF, correlation analysis and synthetic analysis. The research results show that: the summer precipitation distribution in Southwest China is mainly divided into two types: the whole region consistent type and the north-south contrary type. EAP teleconnection patterns and SCA teleconnection patterns have a significant negative correlation with the precipitation in Southwest China during the same period. In the active year (teleconnection indices  $\geq 0.3$  or  $\leq -0.3$ ), the two teleconnection patterns mostly appear in the same phase, and the distribution of the precipitation is consistent with the second mode distribution of the EOF for summer precipitation in Southwest China, showing a north-south contrary distribution in Southwest China. The two types of teleconnections are divided into two configurations, both of which are positive phase (configuration I), and both are negative phase (configuration II). Configuration I, the summer precipitation in Southwest China presents the distribution of "more in the south and less in the north"; configuration II, the distribution of precipitation is opposite to that configuration I, showing the distribution of "more in the north and

less in the south".

**Key words:** Southwest China, Summer Precipitation, East Asia Pacific teleconnection, Scandinavian teleconnection

## 1 Introduction

The East Asia-Pacific (EAP) teleconnection pattern, also known as the Pacific-Japan teleconnection pattern (Pacific-Japan, PJ), was first proposed by Huang et al. (1987) and Nitta et al. (1987). The formation of this teleconnection pattern is related to the anomaly of convective activity over the western Pacific warm pool (Huang and Sun, 1992, 1994). Shi et al. (2008) analyzed the evolution process of EAP in the pre-rainy season in South China and believed that the maintenance and development of EAP teleconnection pattern are related to the Rossby activities in the middle-high latitude. Huang (2004) defined the EAP index according to the activity center of the EAP teleconnection pattern and pointed out that the EAP teleconnection pattern is closely related to the summer climate in East Asia. Cai et al. (2009) pointed out that the EAP teleconnection pattern is closely related to the distribution of summer precipitation in China based on the East Asian atmospheric teleconnection index defined by them. The EAP teleconnection pattern can influence the East Asian summer monsoon and cause summer precipitation anomalies in the middle and lower reaches of the Yangtze River (Min et al. 2005; Lu and Ju, 2006). When the EAP wave train is abnormal, the subtropical high will be stronger to the north, resulting in drought in the Yangtze-Huaihe River basin. (Huang et al. 1990; Lin et al. 1999; Chen et al. 2008). The different distribution of "- + -(+ - +)" in the meridional direction of the EAP teleconnection pattern will promote (suppress) the northward uplift of the western Pacific subtropical high (Yang et al. 2009). Li et al. (2016) pointed out that continuous precipitation occurs in the Yangtze River Basin under the 10 ~ 30 day low-frequency oscillation of EAP teleconnection pattern. Yin et al. (2021) pointed out that the northeast movement of the EAP teleconnection pattern in the activity center

near Japan weakened its connection with summer precipitation in the Yangtze-Huaihe River basin.

The Scandinavian (SCA) teleconnection pattern was first proposed by Barnston et al. (1987), which was obtained by the decomposition of the Eurasian teleconnection pattern. Bueh and Nakamura (2007) analyzed the maintenance mechanism of the SCA teleconnection pattern and pointed out that the two activity centers in North Atlantic and Scandinavia of the upstream part of the SCA teleconnection pattern is maintained by the baroclinic positive feedback action of the transient wave, and the activity center in Siberia of the downstream part is formed and maintained by the energy dispersion of the upstream Rossby wave. Bueh et al. (2008) reached similar conclusions by discussing the abnormal flow pattern in northern Europe in the winter of 2000/2001. Liu et al. (2014) pointed out that the maintenance of the SCA teleconnection pattern is also related to the abnormal convergence (divergence) over the Mediterranean Sea caused by the change of SST in the Indian Ocean. As an important teleconnection pattern in Eurasia, the SCA teleconnection pattern has a significant impact on the temperature and precipitation in Europe (Bueh and Nakamura, 2007; Zveryaev, 2009; Liu et al. 2014), which also has an important impact on climate change in East Asia. Yang et al. (2010a, b) pointed out that the SCA teleconnection pattern is closely related to the precipitation anomalies in winter and spring in Xinjiang, the positive (negative) phase circulation anomalies of the SCA teleconnection pattern can cause more(less) precipitation anomalies in Xinjiang in winter and spring. Lin (2014) pointed out that there is a connection between the SCA teleconnection pattern and the summer precipitation in East Asia, when the SCA teleconnection pattern is in the positive phase, the low pressure in the northern part of East Asia moves northward, resulting in water vapor to be transported to the northwestern part of Northeast Asia, which will significantly reduce the precipitation in North China. Gao et al. (2017) pointed out that there is a close connection between the SCA teleconnection pattern and the westerly zone in summer, and the westerly zone becomes stronger under the negative phase of the SCA teleconnection pattern,

thus, the East Asian shallow trough is located eastward. Yao and Yan (2018) pointed out that the precipitation anomaly in Yunnan in January is closely related to SCA. When SCA is in the positive (negative) phase, the precipitation in January in Yunnan is less (more). Choi et al. (2020) pointed out that the SCA teleconnection pattern in summer plays an important role in the development of heatwaves in East Asia.

According to the current research, it can be seen that the EAP teleconnection pattern and SCA teleconnection pattern have a significant impact on summer climate change in China. However, the precipitation pattern in Southwest China is complex and the spatial distribution varies greatly (Dong et al. 1998; Liu et al. 2002; Ma et al. 2006; Xiong et al. 2012). Summer is also a period of frequent drought and flood disasters in Southwest China (Dai et al. 2015; Deng et al. 2021), summer precipitation anomalies will lead to severe droughts and floods (Lü et al. 2013; Sun et al. 2017). The SCA teleconnection pattern in summer is closely related to subtropical high (Gao et al. 2017), and also has an important influence on the late autumn precipitation in Southwest China (Liu and Liu, 2016, 2017). So, what effect will the EAP teleconnection and the SCA teleconnection have on summer precipitation in Southwest China in Southwest China? Secondly, the climate in Southwest China is jointly affected by the cold and dry airflows in mid and high latitudes and the warm and humid airflows in low latitudes. EAP teleconnection pattern mainly reflects the meridional changes of circulation in East Asia, and the SCA teleconnection pattern reflects the change of zonal circulation in mid and high latitudes propagating eastward from the North Atlantic, SCA teleconnection can propagate eastward to Siberia, which overlaps with EAP teleconnection in Northeast Asia. Then, how do the two types of teleconnections affect the characteristics of summer precipitation in Southwest China under different configurations? Therefore, it is necessary to study the influence of the EAP teleconnection pattern and SCA teleconnection pattern on summer precipitation in Southwest China. This is of great significance to the prediction of the flood season in Southwest China, which is helpful to understand the precipitation mechanism in this region and reduce the losses caused by droughts and floods.

This paper will study the summer precipitation in Southwest China under the influence of teleconnection. Firstly, we analyzed the relationship between the EAP teleconnection pattern and SCA teleconnection pattern and precipitation in Southwest China. Secondly, the distribution form of summer precipitation in Southwest China under different configurations of the SCA teleconnection pattern and EAP teleconnection pattern is analyzed. Finally, the circulation characteristics and water vapor transportation that affect the summer precipitation in Southwest China under different configurations are discussed.

## **2 Data and Analysis Method**

1. The data used include: (1) Daily precipitation observation data of 328 stations in three provinces and one city (Yunnan, Guizhou, Sichuan, Chongqing) in Southwest China from 1970 to 2019, covering a total of 50 years, the station distribution is shown in Figure 1. (2) Monthly reanalysis data from 1970 to 2019 provided by NCAEP/NCAR, including geopotential height field, horizontal wind field, specific humidity, etc., with a horizontal resolution of  $2.5^{\circ}\times 2.5^{\circ}$ , covering a total of 17 layers from 1000hPa to 10hPa in vertical direction. (3) The monthly SCA index provided by CPC/NOAA. The data period is from 1970 to 2019.

In this paper, June, July, and August are selected as summer months.

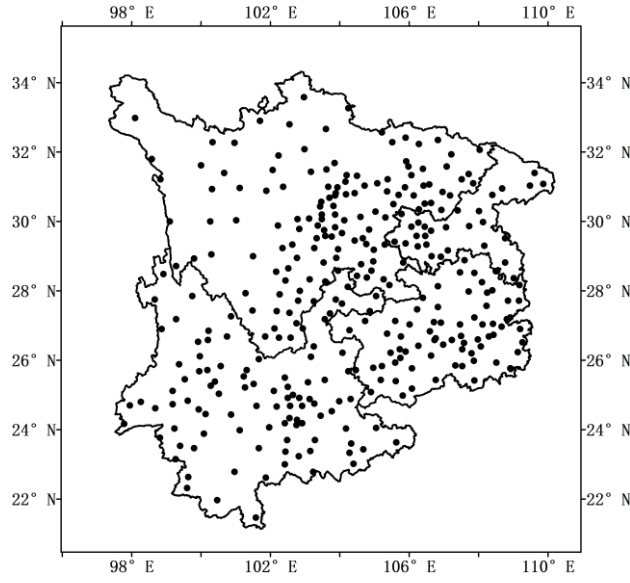


Figure 1 Distribution of 328 precipitation observation stations in Southwest China

2. The calculation of EAP index adopts the definition of Huang (2004):

$$I_{\text{EAP}} = -0.25Z'_s(60^\circ \text{N}, 125^\circ \text{E}) + 0.50Z'_s(40^\circ \text{N}, 125^\circ \text{E}) - 0.25Z'_s(20^\circ \text{N}, 125^\circ \text{E}) \quad (1)$$

In formula (1),  $Z' = Z - \bar{Z}$  means the anomaly processing of the original geopotential height field ( $Z$  is 500 hPa geopotential height,  $\bar{Z}$  means the average climate state);  $Z'_s = Z' \sin 45^\circ / \sin \varphi$  means the zonal standardized processing,  $\varphi$  means the latitude value corresponding to the grid point.

In this paper, the influence of East Asia Pacific teleconnection pattern and Scandinavian teleconnection pattern on summer precipitation in Southwest China is studied by using the methods of empirical orthogonal function decomposition, correlation analysis, regression analysis, and composite analysis.

### **3 Relationship Between SCA Teleconnection Pattern and EAP Teleconnection Pattern and the Summer Precipitation in Southwest China**

#### **3.1 The characteristics of summer precipitation in Southwest China and its correlation with SCA teleconnection pattern and EAP teleconnection pattern**

According to formula (1), the EAP standardized sequence index from 1970 to 2019 is calculated, and the calculation results are consistent with the result of Huang (2004). In order to further demonstrate the spatial distribution characteristics of EAP teleconnection pattern and SCA teleconnection pattern, the teleconnection index and the 500hPa circulation field are used for regression analysis. In Figure 2a, 2b show the regression analysis of EAP, SCA index, and 500 hPa geopotential height anomaly field in summer from 1970 to 2019, which shows the corresponding spatial distribution of these two types of teleconnections, and the shadow means passing 0.05 significance level. The EAP teleconnection pattern presents a "- + -" tripole type meridional distribution from low latitudes to high latitudes in East Asia (Fig. 2a). For SCA teleconnection pattern, there is an obvious positive area in Scandinavia and an obvious negative area in the North Atlantic and Siberia, and it presents a "- + -" zonal wave train from the central-eastern North Atlantic to Lake Baikal in the mid and high latitudes (Fig. 2b). Figure 2c, shows the regression analysis of the average summer precipitation in Southwest China from 1970 to 2019 and the 500 hPa geopotential height anomaly field over the same period. From the figure, it can be seen that there is a "tripole" type distribution similar to EAP teleconnection pattern from low latitudes to high latitudes in East Asia, and also there is also a distribution similar to SCA teleconnection pattern. Therefore, to a certain extent, it shows that the summer precipitation in Southwest China is simultaneously affected by the EAP teleconnection pattern and SCA teleconnection pattern.

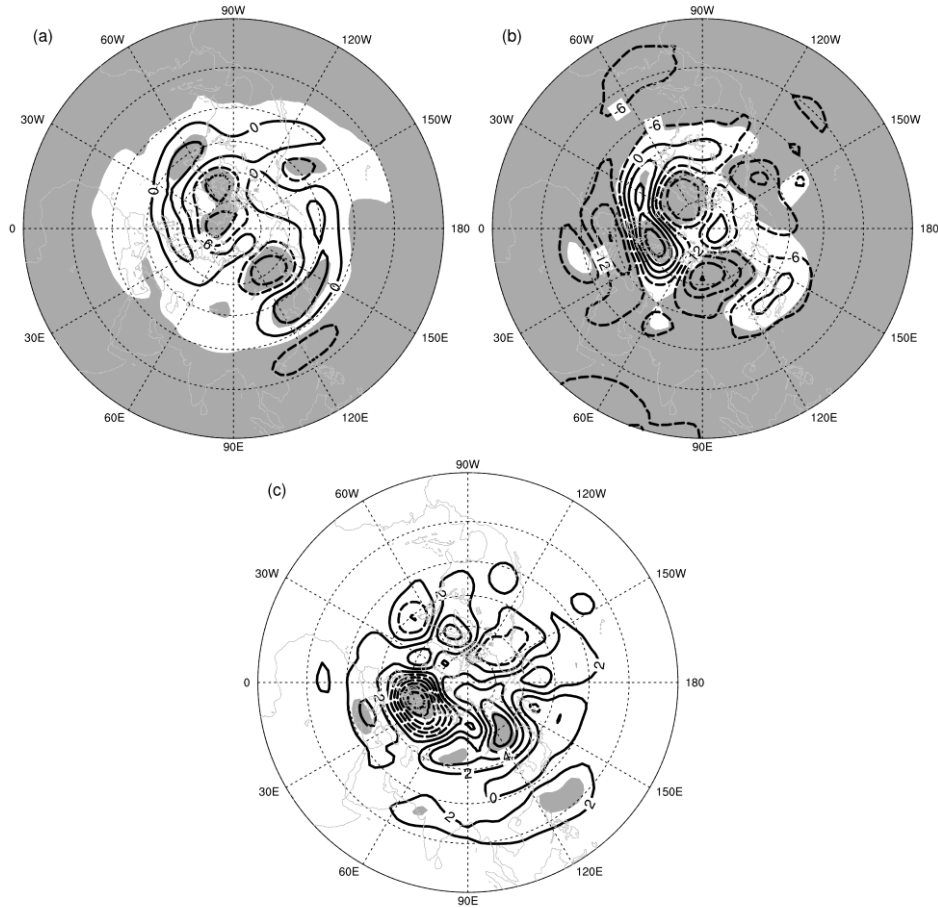


Figure 2 The spatial distribution of EAP index (a) , SCA index (b), and precipitation time series (c) returned to the 500hPa geopotential height field (the shaded area is the area that passed the 0.05 level significance test in descending order)

In order to further explore the relationship between the different configurations of EAP teleconnection pattern and SCA teleconnection pattern and the distribution of summer precipitation in Southwest China, Figure 3 shows the first three modes of summer precipitation EOF in Southwest China, and their variance contributions are 20.15%, 10.88%, and 8.94% respectively. The first mode (Fig. 3a), except for the Sichuan Basin, mainly presents a consistent distribution characteristic in the whole region, with the positive center located in the central part of Guizhou. The second model (Fig. 3b) shows the opposite distribution characteristic of precipitation in the north and south along 27°N. The third mode (Fig. 3c) shows a more obvious difference in east-west distribution, the negative area is located in the Sichuan Basin and Yunnan area, and the positive area is mainly located in Chongqing and Guizhou.

After analyzing the correlation between the time coefficients corresponding to the three modes and the EAP and SCA indices, we got the result as shown in Table 1, the EAP teleconnection index is significantly negatively correlated with the time coefficients of the first three modes, and the correlation with the second modal time coefficient is the strongest, which is -0.411. The SCA teleconnection index is also significantly negatively correlated with the first and second modal time coefficients, and the correlation with the second modal time coefficient is the strongest, which is -0.460. At the same time, the correlation between the two types of teleconnections and the second mode time coefficient is stronger than that of the precipitation time series of the same summer. Thus, it can be seen that the EAP teleconnection pattern and SCA teleconnection pattern are mainly related to the distribution form of the second mode of summer precipitation in Southwest China, that is, precipitation is distributed in reverse from north to south.

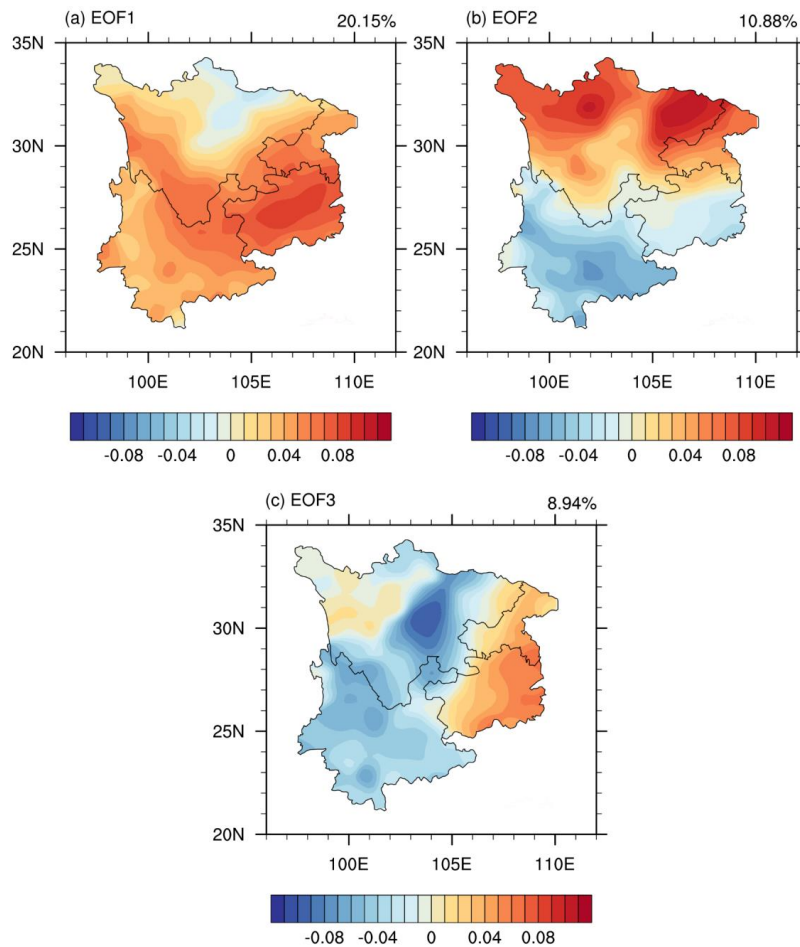


Figure 3 The spatial distribution characteristics of the first three modes of summer precipitation EOF in Southwest China from 1970 to 2019

Table 1 the Correlation between the two patterns of teleconnection indexes, the time series of summer precipitation and the first three modal time coefficients of EOF (\*\* means it is significant at the 0.01 level, \* means it is significant at the 0.05 level)

	PRE	PC1	PC2	PC3
EAP	-0.299*	-0.341*	-0.411**	-0.304*
SCA	-0.385**	-0.344*	-0.460**	-0.022

The spatial distribution of the correlation between the EAP teleconnection pattern and SCA teleconnection pattern and the summer precipitation in Southwest China is further calculated. Both the SCA teleconnection pattern and EAP teleconnection pattern present a “positive in the south and negative in the north” correlation with the summer precipitation in Southwest China, and the summer precipitation in the north of Southwest China has a significant negative correlation with the two teleconnection patterns (Fig. 4). Figure 4a, the negative correlation areas mainly located in western Sichuan Plateau and Guizhou, Chongqing, and eastern Sichuan in the east of Southwest China. Figure 4b, the distribution is consistent with that in Figure 4a, but the negative correlation in Guizhou did not pass the 0.05 significance test. Therefore, if the EAP teleconnection is in a positive phase, when the distribution is "- + -", the precipitation in the north of Southwest China is less, when the distribution is "+ - +", the precipitation is more in the north of Southwest China. The relationship between the positive and negative phase changes of the SCA teleconnection pattern and the summer precipitation in Southwest China is consistent with that of the EAP teleconnection pattern, but the strength of correlation and the significance area are different. At the same time, in the two types of teleconnection patterns, the Sichuan basin area shows the opposite correlation with its east and west areas, indicating that the mechanism of summer precipitation in the basin area is different from its surrounding areas.

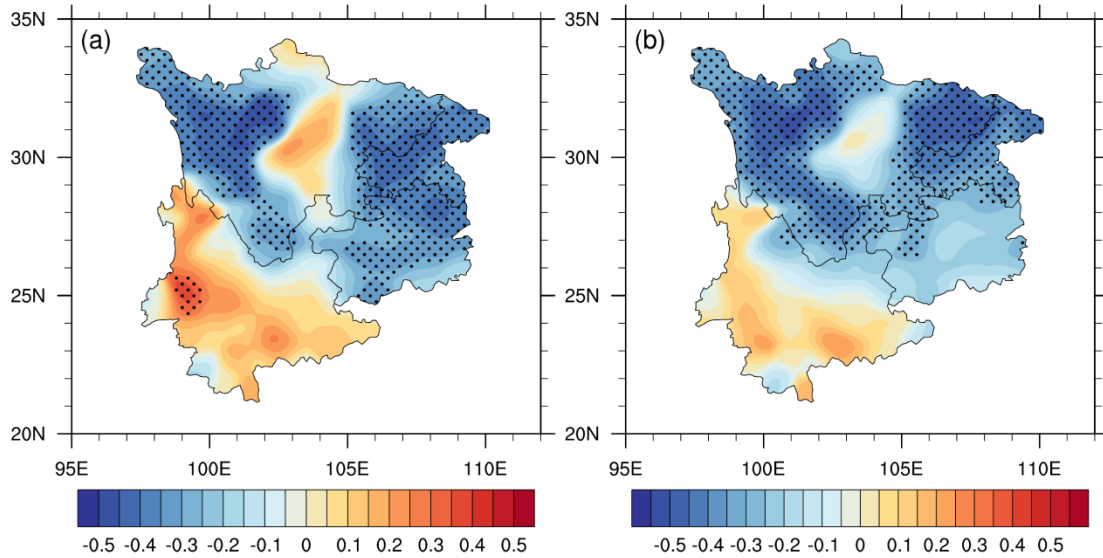


Figure 4 The spatial distribution of the correlation between Scandinavian teleconnection pattern (a) and East Asia-Pacific teleconnection pattern (b) and summer precipitation in Southwest China (the dotted area is the area passing the significance test of 0.05 level)

The above analysis shows that the EAP teleconnection pattern and SCA teleconnection pattern are closely related to summer precipitation in Southwest China. However, the EAP wave is presented as the meridional wave train from low latitude to high latitude, and the SCA wave is presented as the zonal wave train from west to east in middle and high latitude. How they interact and then affect summer precipitation in Southwest China will be the following research work in this paper.

### **3.2 Different configurations of SCA teleconnection pattern and EAP teleconnection pattern and their precipitation distribution characteristics**

From the EAP teleconnection standardized sequence index in the summer of 1970 – 2019 and the SCA teleconnection standardized sequence index provided by CPC/NOAA (Fig. 5), it can be seen that both EAP and SCA indices have the characteristics of interannual and interdecadal variations. There is a significant turning point from positive to negative for the EAP index and SCA index in the late 1970s, and the interdecadal variation weakens, and the inter-annual variation strengthens. In this paper, the SCA teleconnection pattern and EAP teleconnection pattern are divided into positive (negative) phase active years by selecting teleconnections index greater

than (less than) 0.3 times the standard deviation. According to the statistical results of the past 50 years, the occurrence times of the same phase active years of the two types of teleconnection are 14 years in total, and the occurrence times of antiphase active years are 6 years, active years of the same phase account for 70% of the total active years, it can be seen that EAP and SCA mainly appear in the same phase. Therefore, the following part of this paper mainly analyzes the interaction between the two types of teleconnection in the same phase and its influence on summer precipitation in Southwest China. The two configurations of the EAP teleconnection pattern and SCA teleconnection pattern are shown in Table 2: (1) SCA and EAP are both in the positive phase, (2) SCA and EAP are both in the negative phase.

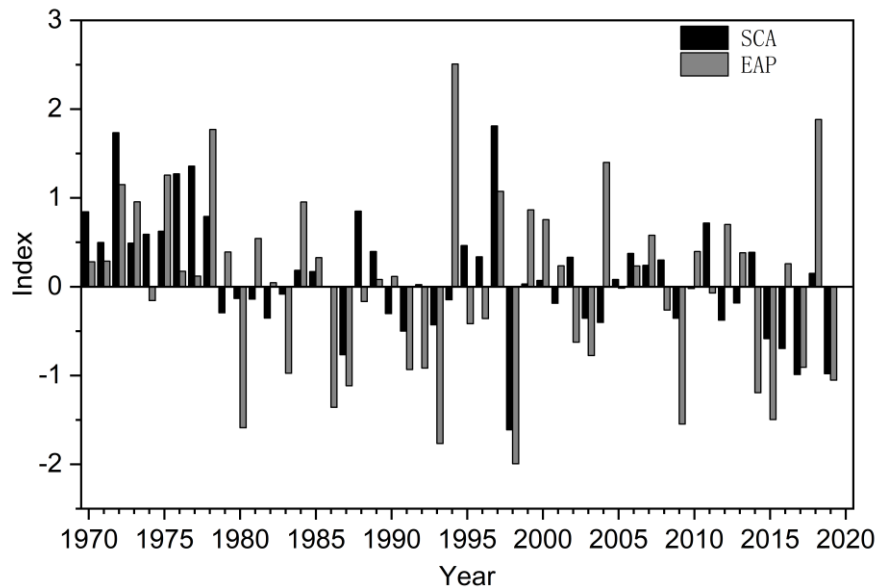


Figure 5 Scandinavian and East Asia-Pacific Teleconnection Index Time Series

Table 2 Corresponding years under different configurations of SCA and EAP indexes

	SCA	EAP	Year				
I	+	+	1972	1973	1975	1978	1997
			1987	1991	1993	1998	2003
II	-	-	2009	2015	2017	2019	

Figure 6 shows the spatial distribution of summer precipitation anomalies in Southwest China under two different configurations. Under configuration I (Fig. 6a), when both EAP teleconnection pattern and SCA teleconnection pattern are in a

positive phase, the summer precipitation in Southwest China shows the distribution characteristics of “less in the north and more in the south”. There is more precipitation in Sichuan, Chongqing, Guizhou, less precipitation in Yunnan, and less precipitation too in the southernmost region of Yunnan. Under configuration II (Fig. 6b), when both the EAP teleconnection pattern and SCA teleconnection pattern are in the negative phase, the precipitation distribution is opposite to that of the configuration I, showing the distribution characteristics of "more in the north and less in the south". The above characteristics are similar to the spatial distribution characteristics (Fig. 3b) and correlation distribution (Fig. 4) of the second mode of EOF. Under the two configurations, the changes in Sichuan Basin are opposite to those in its east and west regions, which are also consistent with the changes mentioned above. Therefore, it can be seen that the summer precipitation distribution under the different configurations of EAP teleconnection pattern and SCA teleconnection pattern can reflect the spatial characteristics of summer precipitation anomalies in Southwest China to a certain extent.

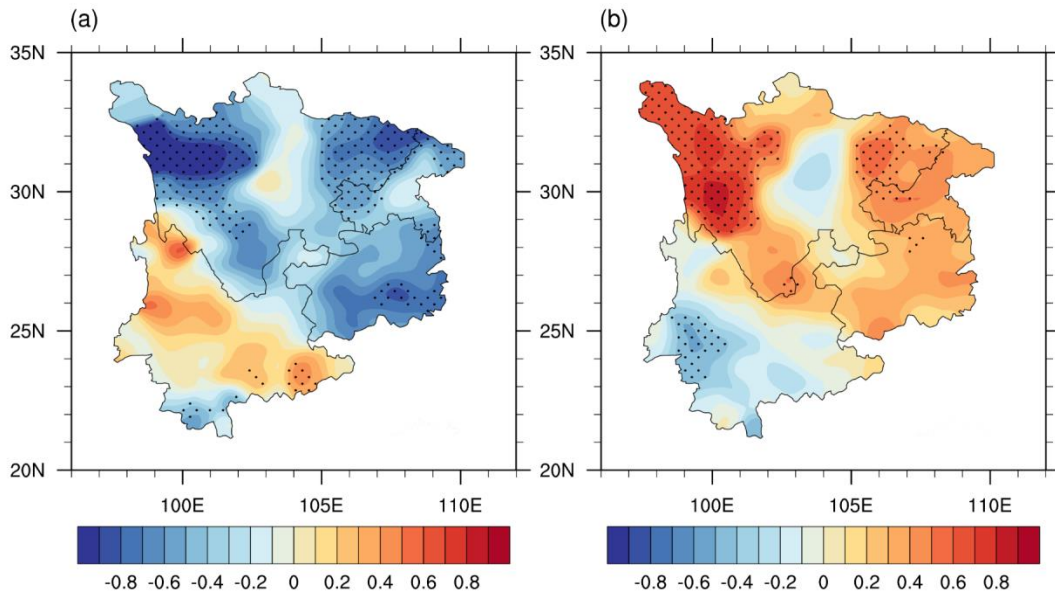


Figure 6 Anomalies Distribution of summer precipitation in Southwest China under different configurations of SCA and EAP indices (a: SCA(+)/EAP(+) b: SCA(-)/EAP(-) c: SCA(+)/EAP(-), the dotted area is the area that passed the 0.05 level significance test)

## **4 Effects of Different Configurations of SCA Teleconnection Pattern and EAP Teleconnection Pattern on Summer Precipitation in Southwest China**

The relationship between the two types of teleconnection and summer precipitation in Southwest China is discussed above. By analyzing the anomalies changes of geopotential height field, wind field, water vapor transport, and vertical velocity, this paper will explore the causes of the difference in precipitation distribution in Southwest China under the two different configurations of teleconnection pattern.

### **4.1 Analysis of atmospheric circulation characteristics under different configurations**

The change of the westerly zone affects the precipitation in the mid and low latitudes (Yin and Li, 2013), and the abnormal disturbance of the westerly zone circulation causes the drought in Yunnan (Yang et al. 2012). Figure 7 shows the 200hPa anomalies of zonal wind fields under two configurations. Under Configuration I (Fig. 7a), there is an obvious westerly zone from the Ural Mountains to the Okhotsk Sea, and its intensity is relatively stronger, which is not conducive to the southward movement of cold air in high latitudes. Under configuration II (Fig. 7b), there are negative anomaly areas in mid and high latitudes, the intensity of the westerly zone is weaker, and the meridional circulation is enhanced, which is conducive to the convergence of cold air in high latitudes southward and warm and humid air to produce precipitation.

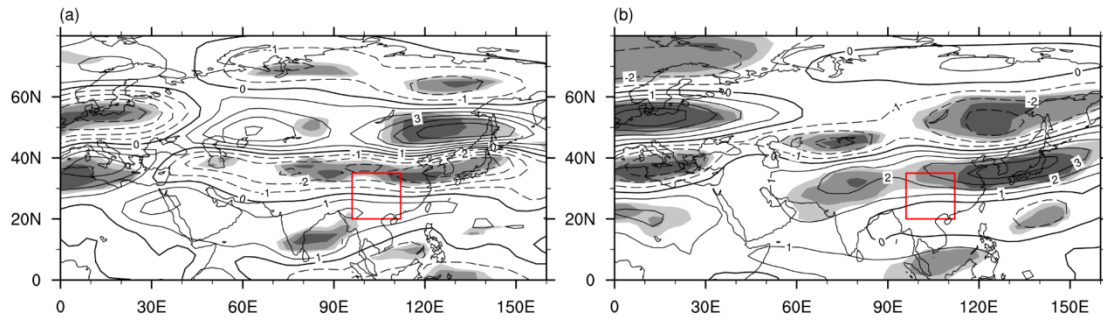


Figure 7 The 200hPa anomalies of zonal wind distribution under different configurations of the two teleconnections (a: SCA(+)/EAP(+) b: SCA(-)/EAP(-), the shaded area is the area that passed the 0.01, 0.05, and 0.1 level significance test in descending order, and the red box part is Southwest China region)

Figure 8 shows the 500hPa anomalies distribution of geopotential height field under different configurations, and figure 9 shows the spatial distribution map of 850hPa wind field anomaly under different configurations. When the two teleconnection patterns belong to configuration I, the zonal circulation situation of "+-" form appears in high latitudes, and the meridional distribution of "-+-" form appears in East Asia from low latitudes to high latitudes (Fig. 8a). It can be seen that SCA zonal wave train and EAP meridional wave train are superimposed in Lake Baikal and Northeast Asia, resulting in the enhancement of negative anomalous circulation. When the EAP index is positive and the wave train is distributed as "- + -" form, the subtropical high will jump northward obviously (Yang et al. 2009). The circulation situation of SCA and EAP superposed each other promotes the development of positive anomalous circulation in the mid-latitudes of East Asia, and the strengthen of the southerly airflow in the west of anticyclone circulation in the mid-latitudes of East Asia. This circulation situation is conducive to the northward of subtropical high. The change of subtropical high has an important influence on summer precipitation in Southwest China (Tao and Wei, 2006; Wu and Wang, 2006; Li, 2013; Yan and Zi, 2021), when the subtropical high is northward, the cold air from the north to the south weakens, the precipitation in Southwest China decreases, the easterly wind in the north of Southwest China strengthens, and Southwest China airflow weakens. The warm and humid airflow in Southwest China reaches Yunnan

and merges with the easterly airflow to form a cyclonic circulation (Fig. 9a), which is conducive to the formation of the precipitation distribution of "more in the south and less in the north" in Southwest China.

In Configuration II, the circulation situation at 500hPa is opposite to that in configuration I (Fig. 8b). the distribution of zonal circulation in the high-latitude region is transformed to " - + " form, while the circulation situation in the East Asian region is in the form of obvious EAP negative phase distribution. The superposition effect of the SCA wave train and EAP wave train in Lake Baikal and Northeast Asia is more significant. The two positive anomaly centers merge to form a large-scale positive value area from the west of Lake Baikal to Northeast Asia. The mid-latitude of East Asia becomes a negative anomaly area. Under this circulation situation, the subtropical high is located southward. In the mid and high latitudes, there is a large negative anomaly area near the Ural Mountains and an obvious positive anomaly area from Lake Balkhash to East Asia with obvious trough ridge and strong meridional transport, which is conducive to the southward movement of cold air. The subtropical high is located in the south, Southwest China is located in the northwest side of the subtropical high, the southwest airflow is stronger and the precipitation in Southwest China increases. In the corresponding 850hPa wind field (Fig. 9b), the cyclonic circulation anomalies in the low latitudes of East Asia enhanced the southwest airflow transport, and the anticyclonic circulation in the middle latitudes further transported the cold air in the high latitudes to the South. The cold air from the north and the warm and humid air from the south converge in the north of Southwest China, and the precipitation increases, resulting in a precipitation distribution of "more in the north and less in the south".

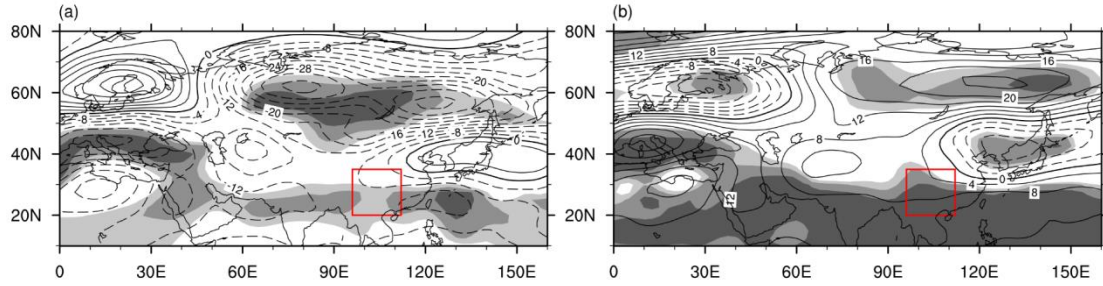


Figure 8 The anomaly distribution of 500hPa height field under different configurations of two teleconnections (a: SCA(+)/EAP(+) b: SCA(-)/EAP(-), the shaded part is the area passing the level significance test of 0.01, 0.05, and 0.1 in descending order, and the red box part is Southwest China region)

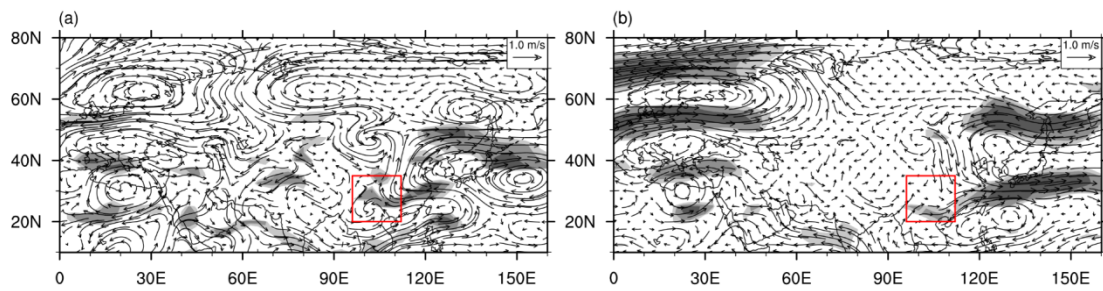


Figure 9 The anomaly distribution of 850hPa wind field under different configurations of two teleconnections (a: SCA(+)/EAP(+) b: SCA(-)/EAP(-), the shaded area is the zonal wind passing the level significance test of 0.05, and the red box part is Southwest China region)

## 4.2 Analysis of water vapor transport in different configurations

Some research pointed out that the water vapor transport in East Asia mainly comes from the water vapor from the Indian Ocean to the Bay of Bengal, followed by the water vapor from the Pacific Ocean. The Tibet Plateau has the effect of diverting the south water vapor eastward. (Miao et al. 2005; Zhou et al. 2008).

Li (2010) also pointed out that the main channels affecting the water vapor transport in eastern Southwest China are the Indian Ocean water vapor transport channel and the Pacific water vapor transport channel. Figure 10 shows the water vapor flux and water vapor flux divergence anomaly distribution in the whole layer under different configurations. It can be seen from the figure that under Configuration I (Fig. 10a), the subtropical high is northerly, and Southwest China water vapor transport in entire Southwest China is weakened. In the low latitude region, the water vapor transport is mainly characterized by the zonal transport to the south of 20 ° N.

One conveyor belt extends from the Arabian Sea to the east, crossing the Indian Peninsula and the Bay of Bengal and entering the Indochina Peninsula and the South China Sea. The other conveyor belt transports westward from the equatorial region of northern New Guinea, changes direction at the ocean surface west of the Philippine Islands, merging with the previous water vapor transport channel, and then changing directing at the ocean surface east of the Philippine Islands, and transporting water vapor to Southwest China from the Pacific channel. After entering China and reaching the middle and lower reaches of the Yangtze River, the water vapor transported from the Pacific is divided into two branches, and the intensity decreases. One continues to move west to Southwest China, the other is affected by the subtropical high and turns northward to North China. At this time, the water vapor transport in the north of Southwest China is divergent, which is not conducive to precipitation. But the water vapor transported from the Pacific Ocean to Southwest China intersects with the water vapor transported from the Bay of Bengal to Southwest China in the south of Southwest China, thus forming a water vapor convergence area, which is conducive to precipitation in the south of Southwest China.

Under Configuration II (Fig. 10b), the water vapor is mainly transported to the southwest through the water vapor channels south of the Tibetan Plateau and the northern Bay of Bengal. The water vapor in the low latitudes presents an obvious zonal characteristic from west to east, it is transported from the western Pacific to west, turns over the Indian Ocean, and transports to Southwest China through the Bay of Bengal. The other branch is transported from eastern Europe to the west and through the southeast side of the Tibet Plateau to Southwest China. Secondly, there is a water vapor convergence center in the Korean Peninsula. The water vapor in the west side of the water vapor convergence area is transported from north to south and intersects with the water vapor from the southeast side of the Tibet Plateau to the Southwest China region. A strong water vapor convergence is formed in the central and northern parts of the Southwest China region, which is beneficial to precipitation. The results are consistent with the spatial distribution results of precipitation under

configuration II. There is more precipitation in the western Sichuan Plateau, Guizhou, and eastern Sichuan except for Yunnan. Therefore, when the EAP teleconnection pattern and SCA teleconnection pattern are both in the positive phase, the water vapor transport from the western Pacific to the east is dominant in Southwest China. When the EAP teleconnection pattern and the SCA teleconnection pattern are both in negative phases, the southwest water vapor transport is dominant.

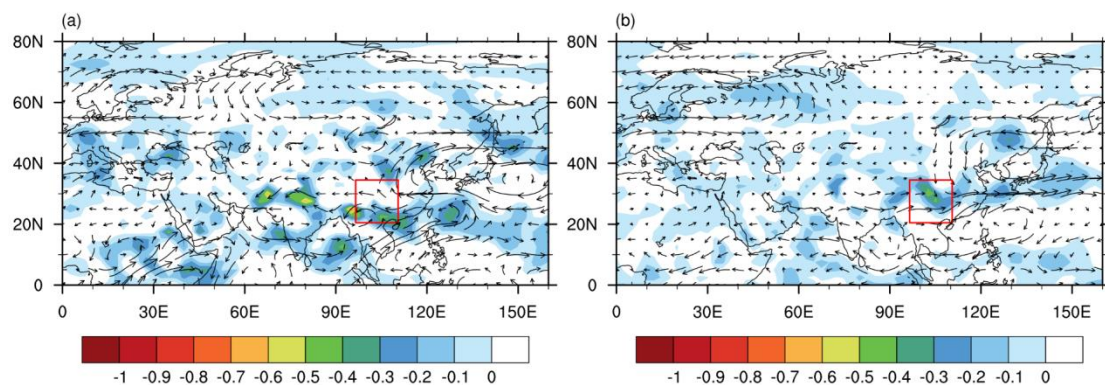


Figure 10 The water vapor flux (unit:  $Kg / (m \cdot s)$ ) and its divergence anomaly (shadow, unit:

$10^{-6} Kg / (m^2 \cdot s)$ ) of the whole layer under two different configurations of teleconnection

patterns( a: SCA(+)/EAP(+) b: SCA(-)/EAP(-))

### 4.3 Analysis of vertical profile under different configurations

In order to further explore the north-south distribution characteristics of precipitation under different configurations in Southwest China, the zonal-height profiles of zonal wind, meridional wind, and vertical velocity under different configurations are given below (Fig. 11). In the zonal wind profile, the configuration I shows that the zonal wind is a negative anomaly area in Southwest China to the north of  $20^{\circ}N$ , mainly easterly wind. The area to the south of  $20^{\circ}N$  is a positive anomaly area, mainly westerly wind, so the western wind has a weaker influence in Southwest China, the water vapor in Southwest China mainly comes from the Pacific (Fig. 11a). The southwest water vapor transport is dominant in the channel of average water vapor transport in summer in Southwest China (Li, 2013). Zhang and Wu et al. (2021), therefore, in Configuration I, although the water vapor transport by the easterly winds

in the Pacific is strong, the water vapor transport in Southwest China weakens, the overall water vapor transport in Southwest China weakens, causing less precipitation in this region. But the south of Southwest China is also affected by the weaker southwest airflow, there was a concentration of water vapor and the precipitation increased in the southern part of the Southwest China region. The zonal wind profile distribution of Configuring II is reversed from Configuring I at mid and low latitudes, Southwest China is dominated by westerly wind (Fig. 11b), and the southwest water vapor transport in Southwest China is enhanced, which increased the precipitation in Southwest China.

In the meridional wind profile of configuration I, the southerly wind component is dominant in the middle and upper layers, and the northerly wind component is dominant in the lower layer in Southwest China. The airflow rising area is about  $24^{\circ}$  N and the airflow sinking area is about  $30^{\circ}$  N (Fig. 11C). The rising movement is conducive to precipitation. Therefore, the precipitation in the south of Southwest China increases, and that in the North decreases. In Configuring II, the north wind component is dominant in the mid and low latitudes of Southwest China, the region to the north of  $30^{\circ}$  N is a negative anomaly region and the south wind component is dominated (Fig. 11d). It is affected by the updraft near  $30^{\circ}$  N, so the precipitation in the north of Southwest China increases.

From the vertical velocity profile (Fig. 11e), it can be seen that the low-layer to high-layer in the north of Southwest China are under the control of abnormal updraft, which is easy to produce precipitation. However, the northern part of Southwest China to the north of  $24^{\circ}$  N is mainly controlled by the downdraft, which is not easy to produce precipitation, and the results are consistent with the results of precipitation distribution in the configuration I (Fig. 6a). In configuration II, the distribution of vertical velocity in zonal direction is opposite to that in the configuration I (Fig. 11f), and the northern part of Southwest China is a negative area ( $\omega < 0$ ), which is controlled by the updraft, and the southern part of Southwest China is a positive area ( $\omega > 0$ ), which is controlled by the downdraft, thus forming the precipitation

distribution of “more in the north and less in the south” in configuration II (Fig. 6b).

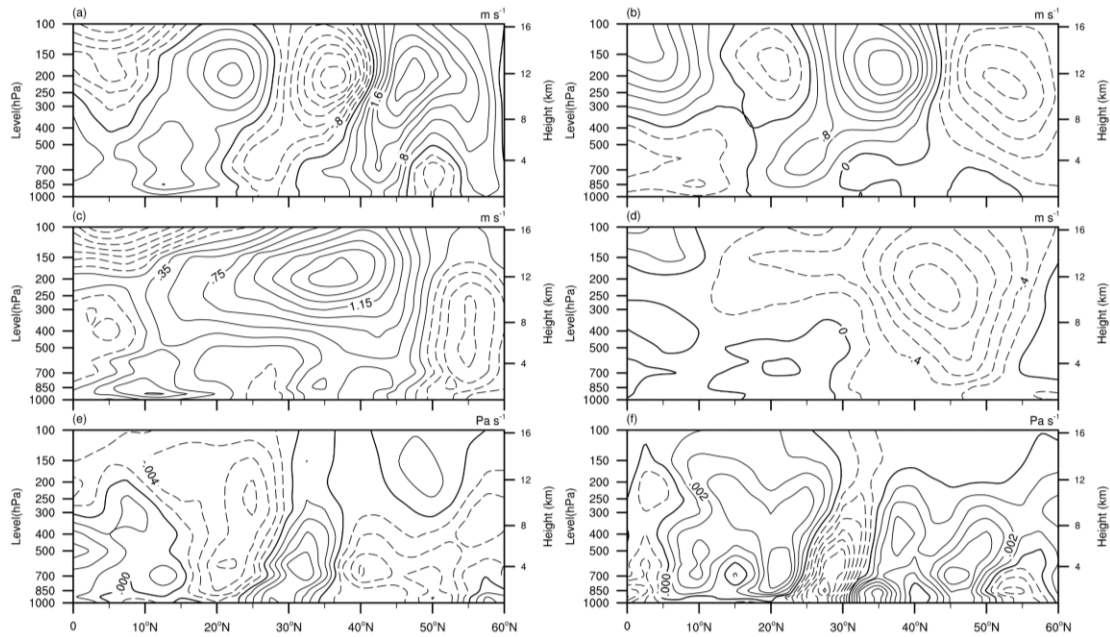


Figure 11 The zonal-height profiles of zonal wind (a, b), meridional wind (c, d) and vertical velocity (e, f) along  $97.5^{\circ}\text{E}\sim 110.5^{\circ}\text{E}$  in different configurations (configuration I: a, c, e), Configuration II: b, d, f)

## 5 Conclusions

Based on the summer precipitation data and NCEP/NCAR reanalysis data in Southwest China from 1970 to 2019, the situation of summer precipitation in Southwest China was analyzed, and the correlation between summer precipitation in Southwest China and SCA and EAP teleconnections was calculated respectively, it was found that SCA teleconnection pattern and EAP teleconnection pattern were closely related to summer precipitation in Southwest China. According to the teleconnection index, the SCA teleconnection pattern and EAP teleconnection pattern can be divided into two configurations. The interaction between the SCA teleconnection pattern and EAP teleconnection pattern under two configurations and the distribution of summer precipitation in Southwest China under different configurations are explored. Finally, the influence of the two configurations on the summer precipitation distribution in southwest China was studied through the data of the circulation situation, the water vapor transport anomaly, and the vertical velocity,

and the following conclusions were drawn:

(1) EAP teleconnection pattern and SCA teleconnection pattern are mainly related to the spatial distribution of the EOF second mode of summer precipitation in Southwest China, that is, which influences the north-south distribution of summer precipitation in Southwest China. There is a negative correlation between EAP teleconnection pattern and SCA teleconnection pattern and summer precipitation in Southwest China during the same period. When both types of teleconnection are positive (negative) phases, and the precipitation in the north of Southwest China is less (more).

(2) SCA teleconnection pattern and EAP teleconnection pattern mainly appear in the same phase, and their spatial structures show zonal and meridional atmospheric circulation anomalies respectively, the two types overlap in Lake Baikal. Based on the two teleconnection indexes of SCA and EAP, it is divided into two configurations: I (++) and II (--), the summer precipitation in Southwest China shows different distribution characteristics under these two configurations.

(3) In Configuration I, under the influence of the two types of teleconnection, the westerly zone is stronger, and the southward transport of cold air at high latitudes is weaker. The subtropical high position of the western Pacific is northward, and the north of Southwest China is mainly affected by the easterly airflow, and the water vapor mainly comes from the western Pacific. The south of Southwest China is still controlled by southwesterly airflow, and there is a cyclonic circulation in the low-level wind field. The water vapor from the western Pacific and the water vapor from the Bay of Bengal intersect in the south of Southwest China, forming a water vapor convergence. Therefore, there is a precipitation distribution of “more in the south and less in the north”.

(4) In Configuration II: there is high pressure in the northern Balkhash Lake and the Okhotsk Sea in summer. The position of the subtropical high of the western Pacific is southward, and the southwest airflow transport is enhanced, reaching the north of Southwest China, where it intersects with the cold air transported southward,

and the precipitation increases. Therefore, the precipitation in Southwest China shows a distribution of “more in the north and less in the south”.

**Funding** This research was supported by the Second Tibetan Plateau Comprehensive Scientific Research Project (2019QZK010408), the Program of the State Key Laboratory of Severe Weather (2019LASW-B02), the Innovation and Development Program of China Meteorological Administration (CXFZ2021Z010), the Key Research and development Project of Sichuan Province (22ZDYF0826), the Social Development Special Project of Yunnan Provincial Key Research and Development Program (202103AC100028)

## References

- Barnston A G, Livezey R E (1987) Classification, Seasonality and Persistence of Low-Frequency Atmospheric Circulation Patterns. *Monthly Weather Review* 115(6):1083-1126.
- Bueh C, Nakamura H (2007) Scandinavian pattern and its climatic impact. *Quarterly Journal of the Royal Meteorological Society: A journal of the atmospheric sciences, applied meteorology and physical oceanography* 133(629): 2117-2131.
- Bueh C, Shi N, Ji LR (2008) Maintenance Mechanism of the Scandinavian Pattern in Its Positive Phase during 2000/2001 Winter and Its Influence on the Weather over the Northern Part of China. *Plateau Meteorology* 27(1): 76-83.
- Cai XZ, Wen ZZ, Yang YW (2009) Atmospheric teleconnection pattern of East Asian summer monsoon anomaly and its impact on summer rainfall in China. *Journal of the Meteorological Sciences* 2009(1):46-51.
- Chen W, Gu L, Wei K et al (2008) Studies of the dynamic processes of East Asian monsoon system and the quas-stationary planetary wave activities. *Chinese Journal of Atmospheric Sciences (in Chinese)* 32(4):950-966
- Choi N, Lee M I, Cha D H et al (2020) Decadal changes in the interannual variability of heat waves in East Asia caused by atmospheric teleconnection changes. *Journal of Climate*, 2020,

33(4): 1505-1522.

Dai X G, Liu Y, Wang P (2015) Warm-dry collocation of recent drought in southwestern China tied to moisture transport and climate warming. *Chinese Physics B* 24(04):550-558.

Deng CZ, Zhao Y, Kong FY, et al (2021) A Numerical Simulation Study of the Southwest Vortex Mechanism during the "6·30" Heavy Rain Event in Sichuan and Chongqing. *Plateau Meteorology* 40(1): 85-97.

Dong Xieqiong, Duan xu (1998) Climate characteristics and variation tendency of precipitation in the Southwest region of China. *Journal of the Meteorological Sciences* 18(3):239-247.

Gao T, Yu J, Paek H (2017) Impacts of four northern-hemisphere teleconnection patterns on atmospheric circulations over Eurasia and the Pacific. *Theoretical and Applied Climatology* 129(3): 815-831.

Huang RH, Li WJ (1987) Influence of the heat source anomaly over the western tropical Pacific on the subtropical high over East Asia. *Proc. International Conference on the General Circulation of East Asia, Chengdu, China, April 10-15, 40-45.*

Huang RH (1990) Studies on the teleconnections of the general circulation anomalies of East Asia causing the summer drought and flood in China and their physical mechanism[J]. *Chin. J. Atmos. Sci* 14(1): 108-117.

Huang RH, Sun FY (1992) Interannual variation of the summer teleconnection pattern over the Northern Hemisphere and its numerical simulation. *Chin. J. Atmos. Sci* 16(1): 52-61.

Huang RH, Sun FY (1994) Impacts of the thermal state and the convective activities in the tropical western warm pool on the summer climate anomalies in East Asia. *Chinese J. Atmos. Sci* 18(2): 141-151.

Huang G (2004) An index measuring the interannual variation of the East Asian summer monsoon-The EAP index. *Advances in Atmospheric Sciences* 21(1): 41-52.

Li YH, Xu HM, Gao YH et al (2010) The characteristics of moisture transport associated with drought/flood in summer over the east of the southwestern China. *Acta Meteorologica Sinica* 68(6):932-943.

Li YH, Qing JM, Li QG et al (2013) Features of Western Pacific Subtropical High (WPSH) Associated with Drought/Flood in Summer over the Eastern Part of Southwest China. *Journal*

- of Southwest University (Natural Science Edition) 35(3):106-116.
- Li L, Zhai PM, Chen Y et al (2016) Low-frequency oscillations of the East Asia–Pacific teleconnection pattern and their impacts on persistent heavy precipitation in the Yangtze–Huai River valley. *Journal of Meteorological Research* 30(4): 459-471.
- Lin J, He JH, Zhang YY. (1999) Relationship of summer EAP to the rainfall in the middle-lower reaches of the Yangtze River. *Journal of Nanjing Institute of Meteorology* 22(3): 312-320.
- Lin Z (2014) Intercomparison of the impacts of four summer teleconnections over Eurasia on East Asian rainfall. *Advances in Atmospheric Sciences* 31(6): 1366-1376.
- Liu Y, Wang QQ, Cheng ZQ (2002) Regional features of summer rainfall anomaly over Southwest China. *Journal of Nanjing Institute of Meteorology* 25(1):105-110.
- Liu Y, Wang L, Zhou W et al (2014) Three Eurasian teleconnection patterns: Spatial structures, temporal variability, and associated winter climate anomalies. *Climate dynamics*, 42(11-12): 2817-2839.
- Liu Y, Liu YM (2016) Spatial Pattern and Causes of Interannual Variability of Autumn Rainfall in Southwest China. *Chinese Journal of Atmospheric Sciences (in Chinese)*, 40(6): 1215-1226.
- Liu Y, Liu YM. (2017) The impact of the Scandinavian teleconnection pattern on late autumn rainfall in the western region of southwest China. *Climatic and Environmental Research (in Chinese)* 22 (1): 80–88.
- Lü JM, Ju JH, Zhang QY et al (2006) Differences of Influences of Tropical Western Pacific SST Anomaly and Rossby Wave Propagation on East Asian Monsoon in the Summers of 1993 and 1994. *Chinese Journal of Atmospheric Sciences (in Chinese)* 30(5): 977-987.
- Lü AM, Wen YR, Li Y. (2013) Study of the impact of tropical cyclone Akash (0701) over the Bay of Bengal on a heavy rainfall event in Southwest China. *Chinese Journal of Atmospheric Sciences (in Chinese)* 37: 160-170.
- Ma ZF, Peng J, Gao WL et al (2006) Climate Variation of Southwest China in Recent 40 Years. *Plateau Meteor* 25(4): 633-642.
- Miao QJ, Xu XD, Zhang SJ (2005) Whole layer water vapor budget of Yangtze River valley and moisture flux component transform in the key areas of the Plateau. *Acta Meteorologica Sinica* 63(1):93-99.

- Min JZ, Li C, Wu P (2005) A Study of the Relationship Between Summer Tropical Convection over the Western Pacific and the Rainfall in the Middle - Lower Reaches of the Yangtze River. Chinese Journal of Atmospheric Sciences (in Chinese) 29(6): 947-954.
- Nitta T (1987) Convective activities in the tropical western Pacific and their impact on the Northern Hemisphere summer circulation. Journal of the Meteorological Society of Japan. Ser. II 65(3): 373-390.
- Shi N, Bueh C, Ji LR et al (2008) The impact of mid-and high-latitude Rossby wave activities on the medium-range evolution of EAP event in the pre-rainy period of South China. Acta Meteorologica Sinica 66(6):1020-1031.
- Sun XT, Li QQ, Wang LJ (2017) Characteristics of long-cycle abrupt drought-flood alternations in Southwest China and anomalies of atmospheric circulation in summer. Chinese Journal of Atmospheric Sciences (in Chinese) 41(6): 1332-1342.
- Tao SY, Wei J (2006) The Westward, Northward Advance of the Subtropical High over the West Pacific in Summer. Journal of Applied Meteorological Science 17(5):513-525.
- Wu HY, Wang QQ (2006) Analysis on Circulation Characteristic of Precipitation Anomalies in Guizhou Summer. Plateau Meteor 25(06):1120-1126.
- Xiong GJ, Wang SG, Shang KZ et al (2012) Climatic characteristics of summer precipitation in southwest China in the past 50 years. Journal of Lanzhou University (Natural Sciences) 48(4):45-52.
- Yao Y, Yan HM (2018) Analysis on Climatic Causes of Precipitation Anomaly in Yunnan in January. Meteorological Monthly 44(12):1583-1592.
- Yan HM, Zi YC (2021) Characteristics of the Subseasonal-Scale Zonal Movement of Subtropical High in Summer and Its Relationship with Precipitation in Southwest China. Chinese Journal of Atmospheric Sciences (in Chinese) 45(1): 1-20.
- Yang RW, Tao Y, Cao J (2009) A mechanism for the interannual variation of East Asia-Pacific teleconnection wave train in early summer. Acta Meteorologica Sinica 67(3):426-432
- Yang LM, Shi YG, Tang H (2010a) Causes of winter precipitation anomalies in northern Xinjiang. Journal of Applied Meteorological Science 21(4): 491-499.
- Yang LM, Shi YG, Tang H (2010b) Characteristics of Atmospheric Circulation and Water Vapor

- for Spring Precipitation Anomaly in Xinjiang. *Plateau Meteorology* 29(06):1464-1473.
- Yang H, Song J, Yan HM et al (2012) Cause of the Severe Drought in Yunnan Province during Winter of 2009 to 2010. *Climatic and Environmental Research (in Chinese)* 17(3):315-326.
- Yin H, Li YH (2013) Summary of Advance on Drought Study in Southwest China. *Journal of Arid Meteorology* 31(01):182-193.
- Yin XX, Zhou LT, Huangfu JL (2021) Weakened Connection between East China Summer Rainfall and the East Asia-Pacific Teleconnection Pattern. *Atmosphere* 12(6): 704-718.
- Zhang C, Wu SH (2021) An analysis on moisture source of extreme precipitation in Southwest China in summer. *Journal of Natural Resources* 36(5): 1186-1194.
- Zhou XX, Ding YH, Wang PX (2008) Moisture transport in Asian summer monsoon region and its relationship with summer precipitation in China. *Acta Meteorologica Sinica* 66(1):59-70.
- Zveryaev I (2009) Interdecadal changes in the links between European precipitation and atmospheric circulation during boreal spring and fall. *Tellus A: Dynamic Meteorology and Oceanography* 61(1): 50-56.